Circular Dichroism and UV-Resonance Raman Investigation of the Temperature Dependence of the Conformations of Linear and Cyclic Elastin

Zeeshan Ahmed, Jonathan P. Scaffidi, Sanford A. Asher
Department of Chemistry, University of Pittsburgh, PA 15260

Received 4 June 2008; revised 4 August 2008; accepted 4 August 2008
Published online 18 October 2008 in Wiley InterScience (www.interscience.wiley.com). DOI 10.1002/bip.21081

ABSTRACT:

We used electronic circular dichroism (CD) and UV resonance Raman (UVRR) spectroscopy at 204 nm excitation to examine the temperature dependence of conformational changes in cyclic and linear elastin peptides. We utilize CD spectroscopy to study global conformation changes in elastin peptides, while UVRR is utilized to probe the local conformation and hydrogen bonding of Val and Pro peptide bonds. Our results indicate that at 20 °C cyclic elastin predominantly populates distorted β-strand, β-type II and β-type III turn conformations. At 60 °C, the β-type II turn population increases, while the distorted β-strand population decreases. Linear elastin predominantly adopts distorted β-strand and β-type III turn conformations with some β-type II turn population at 20 °C. Increasing temperature to 60 °C results in a small increase in the turn population. © *2008 Wiley Periodicals, Inc. Biopolymers 91: 52–60, 2009.*

Keywords: elastin; UV-resonance Raman spectroscopy; circular dichroism; phase transition; β-turns; distorted β-strand

This article was originally published online as an accepted preprint. The "Published Online" date corresponds to the preprint version. You can request a copy of the preprint by emailing the Biopolymers editorial office at biopolymers@wiley.com

Correspondence to: Sanford A. Asher; e-mail: asher@pitt.edu
Contract grant sponsor: NIH
Contract grant number: RO1 EB002053

INTRODUCTION

In recent years, the unique elasticity and resilience of elastin-based peptides have drawn interest from both the biophysics and material science communities.[1–16] Elastin is an important structural peptide that enables elastic deformations of biological assemblies. Biological motion, for example, is enabled by elastin's unique ability to repetitively and reversibly deform upon stress. We all benefit from the elastic properties of elastin, where, hopefully, our aorta reversibly contracts and expands 10^9 times during our lives. Biochemical, genetic, and structural analysis of elastin fibers has demonstrated that the elastin found in skin, blood vessel walls, and lung tissue is a composite of an amorphous component (elastin) and a microfibrillar component (fibrillin). Elastin mimetic peptide $(VPGXG)_n$, where n is the number of repeat pentamers, is widely used as a model system for studying elastin's remarkable viscoelastic properties.

Over the years, considerable effort has been expended to elucidate the mechanism of elastin's unique elasticity.[3–13,16–25] The elastic properties are thought to be associated with or a consequence of elastin's unusual phase transition behavior, which closely resembles that of the thermal volume phase transition behavior of poly(*N*-isopropylacryamide) (PNIPAM).[26–38] PNIPAM polymers contain both hydrophilic and hydrophobic regions, whose exposure to the aqueous medium may change as the polymer collapses at high temperature. The transition temperature of PNIPAM polymers is determined by a delicate balance between amide–water hydrogen bonding, isopropyl group–water interaction, and van der Waals interactions between the hydrophobic groups.[29]

Elastin exists as a highly mobile expanded chain below a certain characteristic temperature that the elastin literature refers to as the "critical temperature, T_c." Above T_c, the peptide chain adopts a compact conformation resulting in a significantly decreased radius of gyration and reduced chain

mobility.[24] The elastin literature calls this thermal behavior an "inverse temperature transition."[20,39] Just as for PNIPAM,[28,29] the transition temperature of elastin peptides can be tuned by changing the hydrophobicity of the polymer. In the $(VPGXG)_n$ system, we can substitute at the X residue.[40]

The remarkable viscoelastic properties of elastin peptides are thought to arise from weakening of peptide–water interactions at elevated temperatures, which results in a hydrophobic collapse of the peptide.[15,24,39] The balance between enthalpy and entropy determines the critical temperature. Below T_c, the favorable enthalpic contribution from amide–water hydrogen bonds and/or charged side chain–water interactions compensate for the unfavorable entropy arising from solvation of hydrophobic groups.[24] The relative importance of this enthalpy advantage is decreased at higher temperatures. Part of this loss results from increased thermal fluctuations, which weaken peptide–water hydrogen bonds. The loss of water–peptide hydrogen bonding-derived stabilization forces the extended peptide chains to contract to minimize the impact of the unfavorable entropy.[24] Increased liberational entropy[41–44] of the released water molecules reduces the entropic cost of hydrophobic solvation and compensates for the loss of configuration entropy incurred upon elastin's transition.[3,4,22,23]

Unfortunately, there are no high-resolution NMR or X-ray structures of elastin because of the high mobility of the peptide's backbone.[39] This lack of detailed knowledge regarding conformational transitions in elastin has significantly impeded efforts for establishing a clear link between structure and function of elastin peptides. Based on spectroscopic studies, Venkatachalam and Urry[23] proposed that, upon an increase in temperature, the highly mobile peptide chains adopt a rigid, well-ordered β-spiral conformation. A β-spiral is composed of repetitive β-type II turns, which form a helix-like structure without interturn $(i - i + 4)$ hydrogen bonds.[17,22,23,45] This model is supported by NMR and Raman studies.[46] These spectroscopic studies found that the collapsed state of the polymer resembles the structure of cyclic $(VPGVG)_3$ peptide crystallized from a mixed water/D_2O–methanol solvent.[17,18,22,23]

Below T_c, the cyclic peptide exists in a β-type II turn conformation, which at high concentrations precipitates at elevated temperatures, presumably into an ordered β-spiral-like conformation.[23] Reiersen et al.[39] used CD spectroscopy to demonstrate that the transition is independent of chain length. The smallest cooperative unit appears to be the pentamer (VPGXG), indicating that long-range interactions do not play a significant role in elastin's inverse transition. The authors demonstrate that small elastin peptides show a broad transition between 1 and 77 °C, where the CD global minimum (200 nm) decreases with increasing temperature. The temperature-dependent behavior of (VPGVG)-repeat elastin peptides appears to be pH-independent.[39]

While Venkatachalam and Urry's β-spiral model is consistent with some of the spectroscopic studies, it does not agree with studies of tissue-derived, water-swollen elastin fibers, which indicate that elastin collapses to a random coil-like conformation.[47–50] Recent molecular dynamics (MD) simulations by Li et al.[3,4] suggest that the collapsed state of elastin is best described as a "compact amorphous structure." The MD study found that, when starting from an idealized β-spiral conformation at low temperatures, the expanded peptide chain retained significant β-spiral population. At high temperatures, however, β-turns and β-strand-like conformations dominate. These results suggest that the collapsed state of elastin may be best described as a molten globule, where the peptide chain locally adopts a short-range β-spiral-like conformation.[3,4]

In this work, we used CD and UVRR to examine temperature-dependent conformation changes in cyclic and linear elastin. Our results indicate that the cyclic peptide predominantly populates distorted β-strand, β-type II and type III turn conformations. In contrast, linear elastin predominantly populates β-type III turn and distorted β-strand conformations, with a minor β-type II turn population as well.

EXPERIMENTAL

The UV resonance Raman spectrometer has been described in detail elsewhere.[51] Briefly, 2 mW of 204 nm UV light was generated by Raman-shifting the 355-nm third harmonic output of an Nd:YAG laser (Coherent, Infinity) in H_2 gas. These UV pulses were then focused at ~45° from the normal to produce a sub-millimeter spot near the interior surface of a rotating fused silica NMR tube (Wilmad) filled with ~1 ml of the sample solution. A 135° backscattering geometry was used for collecting the Raman scattered light, which was then dispersed by a custom-made subtractive double monochromator onto a back-thinned CCD camera (Princeton Instruments-Spec 10 System).[51]

The 15-residue-long cyclic $(VPGVG)_3$ and linear elastin *GVG*$(VPGVG)_2$*VP* were obtained from the Pittsburgh Peptide Synthesis Facility (PPSF, >95% purity) and used at 1 mg/ml concentrations at pH 7. The cyclic peptide was prepared by cyclization of the linear variant (PPSF, >95% purity). Raman spectra (average of three 5-min spectra) were normalized relative to the peak height of the 0.1*M* perchlorate's 932 cm^{-1} band. Three replicate measurements of separately prepared elastin solutions were recorded to ensure measurement reproducibility. Solution pH was adjusted by adding small aliquots of HCl or NaOH. Temperature-dependent CD spectra (average of 10 spectral accumulations) of similarly prepared solutions (pH ~ 5) at 1 mg/ml were measured on a Jasco-715 spectropolarimeter using a 200 μm path length quartz cell. CD and Raman spectra of linear elastin measured at 20 °C subsequent to the elevated temperature measurements were similar to those measured

prior to the temperature increase, indicating the absence of significant photo- or thermal degradation or irreversible aggregation. The CD spectrum of cyclic elastin shows a slight overall decrease in amplitude after heating. This change likely derives from temperature-induced degassing/bubble formation on cell walls at high temperatures.

RESULTS AND DISCUSSION

Cyclic Elastin

We examined the temperature dependence of cyclic elastin's conformation by measuring the circular dichroism (CD) spectra between 0 and 50 °C (see Figure 1). At 0 °C, the cyclic elastin spectrum shows a negative maxima at ~222 nm, a maximum at ~207 nm, and a global minimum below 200 nm. Previous studies indicate that in elastin peptides the presence of a relatively weak negative maxima at ~222 nm is indicative of the presence of β-type I/III turn conformation, while the maximum at ~207 nm is indicative of a β-type II turn conformation.[24,39,52] It should be noted that typically a negative maxima at 222 nm is associated with either an α-helix- or 3_{10}-helix-like conformation. However, in such cases, the global minimum is located above 200 nm, typically around 205–207 nm.[52–54] In cyclic elastin, the global minimum is located below 200 nm, which indicates a significant random coil population, thus excluding the possibility that the feature at 222 nm arises from either α-helix or 3_{10}-helix-like conformations. These results indicate that the global conformation of cyclic elastin contains significant random coil and β-type II and β-type III turn conformations. As the solution temperature is increased, the global minimum value becomes less negative (see Figure 2). A decreased global minimum is regarded as a hallmark of elastin's inverse temperature transition.[24,55,56] No significant changes are observed in either the 222- or the 207-nm region (see Figure 1).

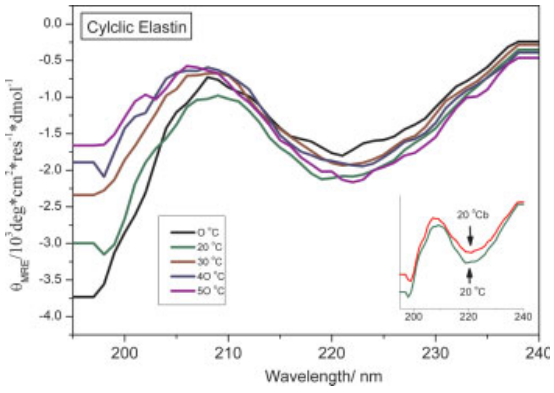

FIGURE 1 Temperature-dependent CD spectra of cyclic elastin. The insert shows the 20 °C CD spectra of cyclic elastin during and subsequent to heating. The CD spectrum subsequent to heating (20 °Cb) shows a slight overall decrease in spectral intensity after heating. This change likely derives from temperature-induced degassing/bubble formation on cell walls at high temperatures.

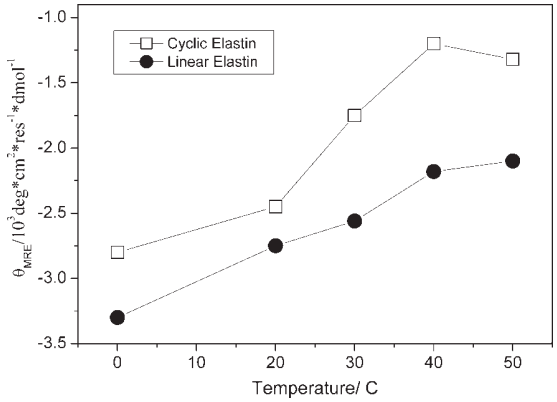

FIGURE 2 Temperature-dependent changes in the mean residue ellipticities of cyclic and linear elastin at 200 nm.

We further probed the temperature dependence of cyclic elastin's backbone conformation by measuring the 204-nm-excited UV resonance Raman spectra at 20 and 60 °C (see Figure 3). There are only three unique types of peptide bonds in elastin, those involving Gly, Pro, and Val. The Raman amide bands significantly differ for these peptide bonds such that they are easily differentiated.

Proline forms a tertiary amide where the pyrrolidine ring side chain loops back onto the backbone. Consequently, Pro

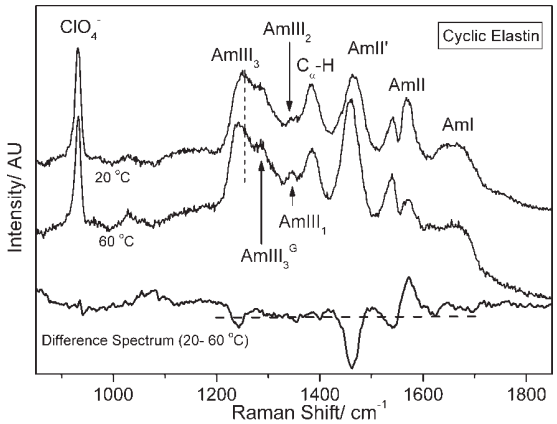

FIGURE 3 The 204-nm UV resonance Raman spectra of cyclic elastin measured at 20 and 60 °C normalized to the intensity of 932 cm^{-1} perchlorate band. The difference spectrum shows temperature-dependent changes in the conformation-sensitive $AmIII_3$ region, as well as intensity changes in the C_α–H_b region. The AmII′p narrows at 60 °C suggesting that the proline peptide bonds adopt a more well-defined conformation at higher temperatures. The trough in the AmII region is an artifact that derives from over-subtraction of the interfering O_2 stretching vibration at 1560 cm^{-1} when the NMR tube contribution was subtracted from the measured spectrum.

peptide bond lacks the amide hydrogen (NH)[57,58] and all the C–N stretching motion is concentrated in a single Raman band labeled AmII′p (amide II′ of proline).[59] The AmII′p band is thought to be sensitive to local conformation and/or hydrogen bonding of the Pro peptide bond.[60–62]

In secondary amides such as those formed by Val and Gly, the amide hydrogen's bending motion (NH_b) couples with the C–N_s and $C_\alpha H_b$ motion, resulting in a complex spectrum that shows multiple bands, namely the AmII (C–N_s with some NH_b at ~1550 cm^{-1}), $C_\alpha H_b$ (1380 cm^{-1}), and various AmIII bands (predominantly C–N_s and NH_b, between ~1200 and 1280 cm^{-1}).

The Gly peptide bond spectrum spectroscopically differs from other nonprolyl peptide bonds due to its two low mass hydrogen atom side chains. The Gly peptide bonds show a single AmIII band at 1284 cm^{-1} ($AmIII^G$) in the amide III region.[63,64] In contrast, the Val peptide bonds show typical Raman spectra in the AmIII region comprising the $AmIII_1$ and $AmIII_2$ bands along with the conformationally sensitive $AmIII_3$ band. The conformation sensitivity of the $AmIII_3$ band arises due to Ψ angle-dependent coupling between NH_b and $C_\alpha H_b$ motions.[65] In extended PPII-like conformations, the NH and $C_\alpha H$ hydrogens are *cis* allowing for a maximum coupling between NH_b and $C_\alpha H_b$ motions. However, in α-helical conformations the NH and $C_\alpha H$ hydrogens are trans which results in insignificant coupling.[65] In Gly, this conformation sensitivity may be lost or decreased due to the presence of two C_α hydrogens ($C_\alpha H_2$), which allows for some coupling with $C_\alpha H$ for all accessible Ψ angles.

Thus, for elastin peptides, we use the AmII′p and the Val $AmIII_3$ bands to probe the conformation and/or hydrogen bonding state of Pro and Val peptide bonds. We utilize CD spectroscopy along with the UVRR information on the Val and Pro peptide bonds to infer Gly peptide bond conformation.

As shown in Figure 4, we deconvoluted the measured 204-nm excited UVRR spectrum into a sum of a minimum number of mixed Gaussian and Lorentzian bands by using the peak-fitting routine in Grams (Galactic Industries Corporation, Grams version 5). The broad ~1660 cm^{-1}AmI band (predominantly C═Os) is composed of two overlapping bands centered at 1674 and 1635 cm^{-1}. Thomas et al. have reported that the amide I region of crystalline cyclic elastin suspended in its mother liquor shows two prominent AmI bands at ~1652 and 1676 cm^{-1}. These authors suggest that both the 1652 and 1676 cm^{-1} AmI bands likely derive from β-type II turn conformations.[46] However, the origin of the frequency difference between these two AmI bands was not discussed.

The two underlying AmI components (1674 and 1635 cm^{-1}) do not result from intrinsically different frequencies for the amide I bands of the Val, Gly, and Pro peptide bonds.

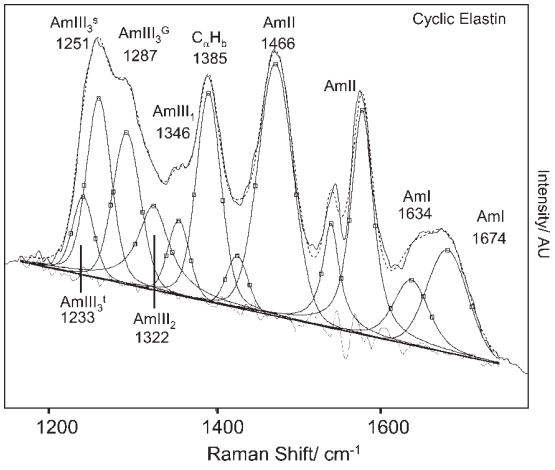

FIGURE 4 Spectral deconvolution of 20 °C 204-nm UV resonance Raman spectra of cyclic elastin with mixed Gaussian and Lorentzian bands. The quality of the fit is evident from the flat residual displayed underneath.

Polyproline peptides show AmI bands in the region between 1640 and 1650 cm^{-1}, while polyglycine peptides show AmI bands at ~1650 cm^{-1}.[64,66,67] The typical nonprolyl, nonglycyl peptide bonds in unfolded peptide conformations typically show a single broad amide I band at 1665 cm^{-1}.[68,69] This frequency spread would not typically result in two overlapping AmI bands at 1635 and 1674 cm^{-1}.

The frequency differences observed for the amide I band either results from significantly different amide bond conformations or from different carbonyl hydrogen bonding. Lazarev et al.[66] reported that the IR absorption spectra of Z-$(Gly_1$-Pro_2-$Gly_3)_4$-OMe peptide in D_2O shows a broad AmI band that appears to be composed of three different AmI components located at 1632, 1650 and 1669 cm^{-1}. These authors attributed the high frequency 1669 cm^{-1} AmI component to the dehydrated/weakly hydrogen-bonded carbonyl of Gly_3.[66] Recently, Spiro and coworkers reported observing a similar high-frequency UVRR AmI band in the PPII (1677 cm^{-1}) and β-sheet (1670 cm^{-1}) conformation of polyK peptide.[70] Boury and coworkers[71] suggest that a similar high-frequency AmI component in Gliadin and Globulin proteins derives from random coil and/or β-turn conformations.

Our CD results indicate that the cyclic elastin peptide predominantly adopts an extended β-strand-like conformation with some β-turn character, discounting the possibility that the high-frequency AmI component derives from β-sheet-like conformations. We therefore conclude that the broad 1635 cm^{-1} AmI component of elastin likely derives from hydrogen-bonded peptide bonds, whereas the 1674 cm^{-1}

component of elastin derives from dehydrated or weakly hydrogen-bonded peptide bonds.

The peptide bond dehydration may correlate with weak amide–amide hydrogen bonding in β-turn-like conformations. X-ray studies of cyclic elastin peptide $(VPGVG)_3$ indicate three β-type II turns. The β-turn spans the VPGV unit and includes a hydrogen bond between the two Val peptide bonds. The other Gly residue appears to serve as a bridge between adjacent turns.[46,72] It is likely that in aqueous solutions, the weakly hydrogen-bonded turn conformation is stabilized against strong peptide–water hydrogen bonding by the bulky β-branched side chains of Val, which are known to restrict water access to the peptide backbone.[73] A lack of significant change in elastin's AmI region at high temperatures (see Figure 2) suggests minimal changes in elastin's hydrogen bonding state. Similar results were reported by Thomas et al., who did not observe any significant change in the amide spectra upon the phase transition.[46] A lack of significant change in the AmI region at high temperatures suggests that the inverse temperature transition of elastin does not significantly impact the hydrogen bonding state of the peptide backbone.

The AmII band at $\sim$1558 cm^{-1} involves C–N stretching with some N–H bending.[69] The trough in the AmII region (see Figure 3) is an artifact from over-subtraction of the interfering molecular oxygen vibration at 1560 cm^{-1}.

The AmII′ band of Pro (AmII′p)[59] located at 1466 cm^{-1} is predominantly a C–N stretch, which is thought to be sensitive to local conformation and/or hydrogen bonding of Pro's peptide bond. The AmII′p downshifts from 1466 to 1460 cm^{-1} and its band width (FWHM) appears to narrow from 50 cm^{-1} to 47 cm^{-1} as the solution temperature is increased from 20 to 60 °C (see Figure 3). We recently demonstrated that the AmII′p band frequency is sensitive to the peptide backbone conformation of proline.[60] The narrowing of the AmII′p band at high temperatures indicates a narrower conformational distribution of the proline peptide bond at 60 °C.

Takeuchi et al.[61] suggested that the AmII′p frequency depends on the hydrogen bonding state of Pro.[61,62] If that were true, then the observed changes in the AmII′p frequency would suggest weakening of amide–water hydrogen bonds at high temperature. However, we see little evidence from the AmI band for peptide bond dehydration.

The $C_\alpha H_b$ band is located at 1385 cm^{-1}. The presence of the resonance-enhanced $C_\alpha H_b$ band is correlated with the presence of non-α-helical conformations.[68,74] In elastin peptides, the $C_\alpha H_b$ intensity derives only from the Val and Gly peptide bonds, although as discussed above, we expect that the impact of Val peptide bond conformational changes on the $C_\alpha H_b$ band intensity would be more than what would occur for the Gly peptide bond.

Table I Conformation Distribution of Linear and Cyclic Elastin

Band Position (cm^{-1})	Ψ Angle (degree)	Conformation
Cyclic elastin		
1251	−35°	β-type III turn
	+165°	Distorted β-strand
1233	0°	β-type II turn
Linear elastin		
1250	−35°	β-type III turn
	+165°	Distorted β-strand
1230	0°	β-type II turn

The amide III region has recently been examined and reassigned.[69,75–78] The $AmIII_1$ band is located at 1346 cm^{-1}, while a weak $AmIII_2$ band is located at $\sim$1322 cm^{-1}. In cyclic elastin, these bands derive only from Val peptide bonds. The 1287-cm^{-1} AmIII band likely derives from glycine peptide bonds. The broad $AmIII_3$ band located at $\sim$1246 cm^{-1} is composed of two overlapping bands at $\sim$1251 and $\sim$1233 cm^{-1} (see Figure 3), which derive from the Val peptide bonds.

Recently, Mikhonin et al.[79] quantitatively demonstrated that the $AmIII_3$ band frequency depends upon the ψ dihedral angle and the hydrogen bonding state of the amide bond.[69,79] Furthermore, Mikhonin and Asher[80] demonstrated that the resonance enhanced AmIII and $C_\alpha H_b$ bands each scatter independently, i.e., there is negligible coupling between adjacent peptide bonds. The UVRR spectra in the AmIII and $C_\alpha H_b$ region can therefore be regarded as a linear sum of individual peptide bonds. Hence, the $AmIII_3$ spectra represents the time-averaged conformation distribution of the peptide bonds.[53,81]

Using Mikhonin et al.'s[79] methodology for correlating the ψ dihedral angle with the $AmIII_3$ band position, we find that the 1251-cm^{-1} band could originate from either a β-type III turn-like conformation ($\psi \sim -35°$) or a distorted β-strand-like conformation ($\psi \sim +165°$, see Table I). The presence of a strong $C_\alpha H_b$ band indicates the existence of significant non-α-helical conformations. As discussed above, the presence of a minimum at 222 nm along with a global minimum below 200 nm in the CD spectra (see Figure 1) indicates that some fraction of cyclic elastin exists in a β-type III turn conformation with a significant content of random-coil like conformation. We therefore conclude that the 1251-cm^{-1} Raman band of cyclic elastin likely contains contributions from both the distorted β-strand and type III turn-like conformations. Similarly, Mikhonin et al.'s data suggest the 1233-cm^{-1} $AmIII_3$ band could originate from either antiparallel β-sheet ($\psi = +135°$) or β-turn ($\psi = 0°$) conformations. Taking our cue from previous elastin studies,[23] we assign the 1233-cm^{-1} $AmIII_3$ band to β-type II turn conformations of the Val peptide bonds.

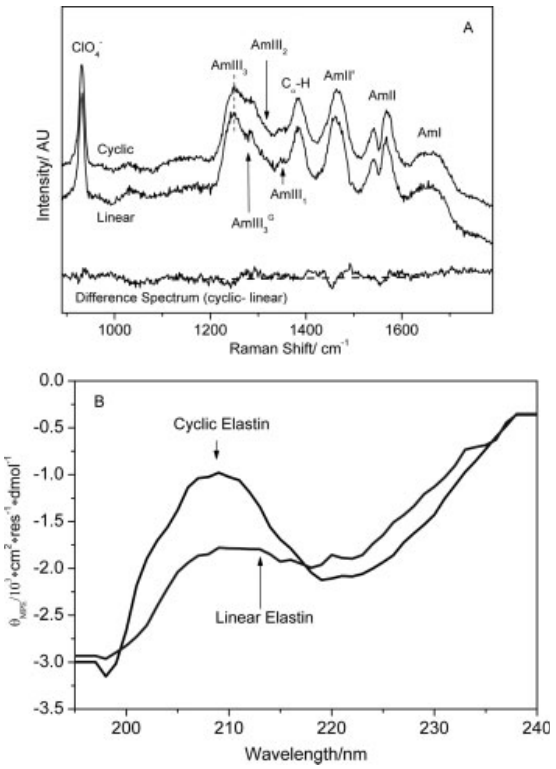

FIGURE 5 (A) 204-nm UV resonance Raman spectra of linear and cyclic elastin at 20 °C and their difference spectra. The featureless difference spectrum indicates that the Val and Pro peptide bonds in cyclic and linear peptides have similar conformations. (B) CD spectra of linear and cyclic elastin at 20 °C. Cyclic elastin shows a less prominent negative feature at ∼207 nm, indicating a greater population of β-type II turns in the cyclic peptide.

The spectra in the $C_\alpha H_b$ and $AmIII_3$ region show some changes in band intensities and position as the temperature is increased from 20 to 60 °C. The frequency of the $C_\alpha H_b$ band is temperature independent.[53,69,82] The $C_\alpha H_b$ band region in the difference spectrum shows a small positive peak; decrease in the $C_\alpha H_b$ band intensity at high temperatures indicates a decrease in the extended state (distorted β-strand) population (see Figure 3). The $AmIII_3$ band appears to show increased band intensity at 60 °C, as indicated by a trough in the difference spectrum at ∼1235 cm^{-1}, which suggests an increased β-type II turn population.

Linear Elastin

At 20 °C, the 204-nm UVRR spectrum of linear elastin (Figure 5A) resembles the 20 °C cyclic elastin spectrum—suggesting that the ensemble conformations of linear elastin's Val and Pro peptide bonds are similar to their counterparts in cyclic elastin. The cyclic and linear elastin peptides have similar sequences, although the cyclic peptide has an extra peptide bond (P-G) due to cyclization of the linear variant and it has no charged groups.

The CD spectrum shows a smaller β-type II turn population for linear elastin than for cyclic peptide as indicated by a less prominent band maximum at ∼207 nm (Figure 5B).[12,24,39] A lack of significant difference in the UVRR spectra of linear elastin versus cyclic elastin suggests that the increased turn population is localized in conformational changes at the Gly peptide bonds. Previous studies suggested that linear elastin's Gly residues are highly mobile.[83]

The CD spectra of linear elastin show little temperature dependence at 222 and 207 nm (see Figure 6), whereas the global minimum below 200 nm becomes less negative with increasing temperature (Figures 2 and 6). The linear slope of the melting curve indicates a non-cooperative transition (see Figure 2). The presence of a negative maxima at ∼222 nm indicates the presence of β-type III turn conformation, while a weak maximum at ∼207 nm is indicative of some β-type II turn conformation.[39] Presence of the global minimum below 200 nm indicates a significant random coil population.[39,52]

The mean residual ellipticity (MRE) of linear elastin at 198 nm of ∼4000 degree cm^2 $residue^{-1}$ $dmol^{-1}$ at 0 °C is significantly smaller than the values reported by Reiersen et al.[39] for short elastin-like peptides. Although, the sequence of peptides in the two studies differs (our peptides have extra Val and Pro residues at the N-terminus), both Reiersen et al.'s and our study show similar spectral features. The relatively small MRE indicates greater β-turn character[39] for our peptide, which likely arises due to the presence of hydrophobic terminal Val and Pro residues. Our CD results indicate that the linear elastin peptide predominantly populates random coil and β-type III turn-like conformations along with a small population of β-type II turns.

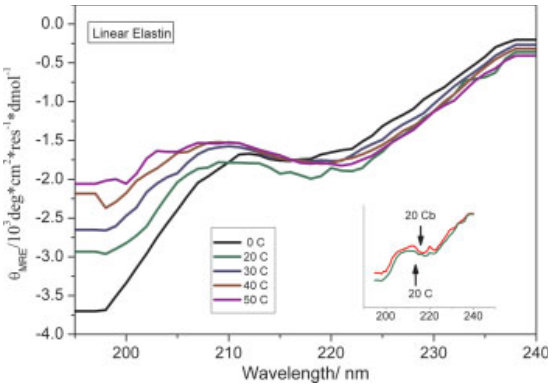

FIGURE 6 Temperature-dependent CD spectra of linear elastin. The insert shows the 20 °C CD spectra of cyclic elastin during and subsequent (20 °C) to heating.

As shown in Figure 7, spectral deconvolution of the UVRR spectrum of linear elastin at 20 °C reveals a similar AmI region as cyclic elastin's with AmI bands at ∼1635 and 1672 cm^{-1}. The trough in the AmII region is an artifact arising due to over-subtraction of the 1560 cm^{-1} molecular oxygen contribution. The AmII′p is located at 1463 cm^{-1}, while the resonance-enhanced $C_\alpha H_b$[68,74] is located at 1383 cm^{-1}. The $AmIII_1$ band is located at 1348 cm^{-1}, while a weak $AmIII_2$ band is located at 1318 cm^{-1}. The $AmIII^G$ is located at ∼1285 cm^{-1}. The conformation-sensitive $AmIII_3$ region (deriving from Val) shows a broad band at ∼1247 cm^{-1} that is likely composed of two overlapping bands located at ∼1250 and ∼1232 cm^{-1} (see Figure 7). According to Mikhonin et al.,[79] the 1232-cm^{-1} band likely derives from β-type II turn-like conformations ($\psi \sim 0°$), while the 1250-cm^{-1} band likely derives from distorted β-strand ($\psi \sim +165°$) and β-type III turn-like conformations ($\psi \sim -35°$, see Table I).

Recently, Ohgo et al.[84] utilized solid-state NMR techniques in conjunction with a statistical analysis of Brookhaven Protein Databank (PDB) to estimate the angular distribution of the two central Val peptide bonds (Val-14 and Val-16) in an isotope-labeled $(VPGVG)_6$ lyophilized peptide. The authors found that Val-14 shows a bimodal distribution of (Φ,Ψ) values at ($-110 \pm 20°$, $130 \pm 20°$) and ($-75 \pm 15°$, $-15 \pm 15°$), which constitutes 70 and 30% of total population, respectively. Val-16 residue adopts the (Φ,Ψ) values of ($-90 \pm 15°$, $120 \pm 15°$). A bimodal distribution was also observed for the central Gly and Pro peptide bonds suggesting that elastin conformation is an ensemble of multiple conformations with some minor β-spiral contribution. Ohgo et al.'s[84] calculated Ψ angle values for Val are similar to our UVRR-derived Ψ angles. The slight differences in Ψ angle values likely derive from increased peptide backbone mobility in our aqueous phase experiment. This suggests that the aqueous conformations observed in our UVRR experiment also occur in the lyophilized solid-state samples of Ohgo et al.[84]

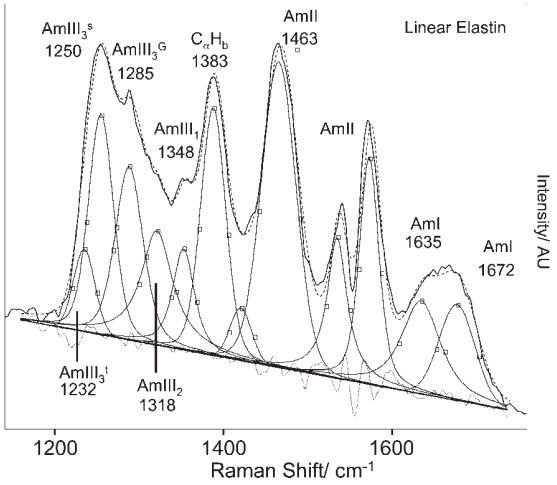

FIGURE 7 Spectral deconvolution of 20 °C 204-nm UV resonance Raman spectra of linear elastin with Gaussian and Lorentzian bands. The quality of the fit is evident from the flat residual.

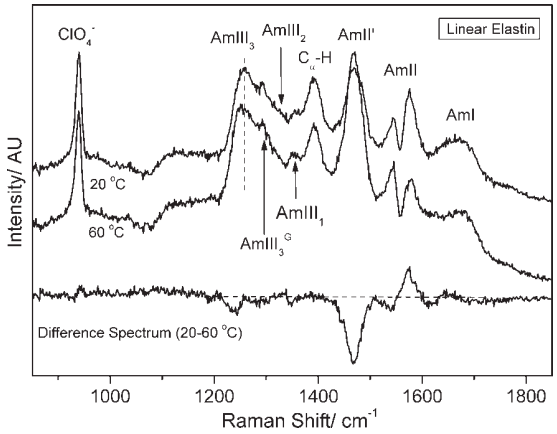

FIGURE 8 The 204-nm UV resonance Raman spectra of linear elastin measured at 20 and 60 °C. The difference spectrum shows narrowing of the AmII′ band width at 60 °C, which is indicative of a transition to a relatively well-defined conformation. The trough in the AmII region is an artifact that derives from over-subtraction of the interfering O_2 stretching vibration at 1560 cm^{-1} when the NMR tube contribution was subtracted from the measured spectra.

As the solution temperature is increased from 20 to 60 °C, the $AmIII_3$ band shows a small increase in band intensity as indicated by a trough in the difference spectrum at ∼1237 cm^{-1}, suggesting an increased β-type II turn population (see Figure 8). The AmII′p band narrows (ΔFWHM = 2 cm^{-1}) as the solution temperature is increased from 20 to 60 °C, suggesting a narrower conformation distribution at 60 °C, although the narrowing in linear elastin (ΔFWHM = 2 cm^{-1}, Figure 8) is just a little less than that in cyclic elastin (ΔFWHM = 3 cm^{-1}, Figure 2). Furthermore, unlike in cyclic elastin, the band position of the AmII′p band in linear elastin remains invariant with temperature. This suggests that unlike the prolines of cyclic elastin, linear elastin's prolines do not undergo a significant conformation change with increasing temperature.

CONCLUSION

We utilize electronic circular dichroism (CD) and UV resonance Raman spectroscopy at 204-nm excitation to examine the temperature dependence of conformational changes in cyclic and linear elastin peptides. We use CD spectroscopy to examine global conformation changes in elastin peptides, while UVRR probes the local conformation and hydrogen

bonding of Val and Pro peptide bonds. Our results indicate that the cyclic peptide predominantly populates distorted β-strand, β-type II, and β-type III turn conformations at 20 °C. At 60 °C, the β-type II turn population increases somewhat, while the distorted β-strand population decreases as indicated by changes in the $AmIII_3$ and $C_\alpha H_b$ regions.

The ensemble population of linear elastin is predominantly β-type III turn and distorted β-strand with some β-type II turn population regardless of solution temperature. Increasing temperature results in a small increase in the β-type II turn population; furthermore, we observe narrowing of the AmII′p band with increasing temperature, which suggests a narrowed conformation distribution at high temperatures.

Our CD spectra of linear elastin versus cyclic elastin indicate a greater β-type II turn population for cyclic elastin. However, the UVRR of cyclic and linear elastin do not show any significant differences. This result suggests that the increased type II turn content of cyclic elastin is likely due to cyclization-induced conformation changes at Gly peptide bonds.

Our results demonstrate that for both cyclic and linear elastin the global conformation changes are predominantly driven by conformation changes at the proline and glycine peptide bonds, whereas the Val peptide bonds show relatively little conformation changes with increasing temperature. However, the Val peptide bonds are probably not mere spectators; they likely play a pivotal role in the inverse temperature transition of elastin peptides.

We find that both the cyclic and linear elastin peptide show a broad AmI band, which is likely composed of two overlapping bands at ~1674 and 1635 cm^{-1}. The 1635 cm^{-1} component derives from hydrogen-bonded peptide bonds, whereas the ~1674 cm^{-1} component likely derives from dehydrated/weakly hydrogen-bonded peptide bonds that are likely engaged in weak intramolecular hydrogen bonding as part of a local β-turn conformation.[46] The weakly hydrogen-bonded β-turn is likely protected against amide–water hydrogen bonds by the bulky β-branched side chains of Val, which are known to shield the peptide backbone from water molecules.[73] The absence of some peptide–water hydrogen bonds in the extended conformation of elastin as compared to typical unfolded peptides such as the XAO peptide, which predominantly adopts a PPII conformation,[69,85–87] reduces the enthalpic advantage of the elastin's extended state over its entropically unfavorable collapsed state and narrows the free energy gap between the extended and collapsed states such that a temperature increase induces the inverse transition.

A lack of significant change in the AmI region at high temperature suggests that the inverse temperature transition of elastin does not significantly impact the hydrogen bonding state of the peptide backbone. Furthermore, small intensity changes in the AmIII and $C_\alpha H_b$ band region indicate that elastin's phase transition is accompanied by only a small conformation change resulting in increased β-turn population. The increased β-turn content does not appear to impact the hydrogen bonding state of elastin. It is likely that the phase transition in elastin peptides is primarily driven by changes in conformation and/or hydration of the alkyl side chains.

The authors would like to thank Prof. D. W. Urry and Konstantin V. Pimenov for helpful discussions.

REFERENCES

1. Alonso, M.; Reboto, V.; Guiscardo, L.; San Martin, A.; Rodriguez-Cabello, J. C. Macromolecules 2000, 33, 9480–9482.
2. Urry, D. W.; Parker, T. M. J Muscle Res Cell Motil 2002, 23, 543–559.
3. Li, B.; Alonso, D. O. V.; Bennion, B. J.; Daggett, V. J Am Chem Soc 2001, 123, 11991–11998.
4. Li, B.; Alonso, D. O. V.; Daggett, V. J Mol Biol 2001, 305, 581–592.
5. Debelle, L.; Alix, A. J. P.; Wei, S. M.; Jacob, M.-P. Eur J Biochem 1998, 258, 533–539.
6. Fernandes, R. J.; Eyre, D. R. Biochem Biophys Res Commun 1999, 261, 635–640.
7. Herrera, B.; Eisenberg, G.; Holberndt, O.; Desco, M. M.; Rábano, A.; García-Barreno, P.; Del Cañizo, J. F. Cryobiology 2000, 41, 43–50.
8. Kim, B.-S.; Nikolovski, J.; Bonadio, J.; Smiley, E.; Mooney, D. J. Exp Cell Res 1999, 251, 318–328.
9. Lapis, K.; Tímár, J. Semin Cancer Biol 2002, 12, 209–217.
10. Lindholt, J. S.; Heickendorff, L.; Vammen, S.; Fasting, H.; Henneberg, E. W. Eur J Vasc Endovasc Surg 2001, 21, 235–240.
11. Nakamura, F.; Suyama, K. Arch Biochem Biophys 1996, 325, 167–173.
12. Reiersen, H.; Rees, A. R. Biochem Biophys Res Commun 2000, 276, 899–904.
13. Robert, L. Semin Cancer Biol 2002, 12, 157–163.
14. Krukau, A.; Brovchenko, I.; Geiger, A. Biomacromolecules 2007, 8, 2196–2202.
15. Tamura, T.; Yamaoka, T.; Kunugi, S.; Panitch, A.; Tirrell, D. A. Biomacromolecules 2000, 1, 552–555.
16. Bressan, G.; Prockop, D. J. Biochemistry 1977, 16, 1406–1412.
17. Khaled, M. A.; Prasad, K. U.; Venkatachalam, C. M.; Urry, D. W. J Am Chem Soc 1985, 107, 7139–7145.
18. Urry, D. W.; Chang, D. K.; Krishna, N. R.; Huang, D. H.; Trapane, T. L.; Prasad, K. U. Biopolymers 1989, 28, 819–833.
19. Urry, D. W.; Harris, R. D.; Prasad, K. U. J Am Chem Soc 1988, 110, 3303–3305.
20. Urry, D. W.; Haynes, B.; Zhang, H.; Harris, R. D.; Prasad, K. U. Proc Natl Acad Sci USA 1988, 85, 3407–3411.
21. Urry, D. W.; Peng, S.; Parker, T. J Am Chem Soc 1993, 115, 7509–7510.
22. Venkatachalam, C. M.; Khaled, M. A.; Sugano, H.; Urry, D. W. J Am Chem Soc 1981, 103, 2372–2379.
23. Venkatachalam, C. M.; Urry, D. W. Macromolecules 1981, 14, 1225–1229.

24. Urry, D. W. J Phys Chem B 1997, 101, 11007–11028.
25. Urry, D. W.; Peng, S.; Xu, J.; McPherson, D. T. J Am Chem Soc 1997, 119, 1161–1162.
26. Debord, S. B.; Lyon, L. A. J Phys Chem B 2003, 107, 2927–2932.
27. Ding, Y.; Ye, X.; Zhang, G. Macromolecules 2005, 38, 904–908.
28. Reese, C. E.; Mikhonin, A. V.; Kamenjicki, M.; Tikhonov, A.; Asher, S. A. J Am Chem Soc 2004, 126, 1493–1496.
29. Wang, J.; Gan, D.; Lyon, L. A.; El-Sayed, M. A. J Am Chem Soc 2001, 123, 11284–11289.
30. Wang, X.; Wu, C. Macromolecules 1999, 32, 4299–4301.
31. Hoare, T.; Pelton, R. Langmuir 2004, 20, 2123–2133.
32. Hu, T.; You, Y.; Pan, C.; Wu, C. J Phys Chem B 2002, 106, 6659–6662.
33. Jones, C. D.; Lyon, L. A. Macromolecules 2003, 36, 1988–1993.
34. Kunugi, S.; Kameyama, K.; Tada, T.; Tanaka, N.; Shibayama, M.; Akashi, M. Braz J Med Biol Res 2005, 38, 1233–1238.
35. Li, C.; Bergbreiter, D. E. In Chemical Industries, Vol. 89: Catalysis of Organic Reactions; Morrell, D. G., Eds.; Marcel Dekker: New York, 2003; pp 545–550.
36. Zhu, P. W.; Napper, D. H. J Colloid Interface Sci 1996, 177, 343–352.
37. Zhu, P. W.; Napper, D. H. J Phys Chem B 1997, 101, 3155–3160.
38. Zhu, P. W.; Napper, D. H. Phys Rev E Stat Phys Plasmas Fluids Relat Interdiscip Topics 2000, 61, 6866–6871.
39. Reiersen, H.; Clarke, A. R.; Rees, A. R. J Mol Biol 1998, 283, 255–264.
40. Luan, C. H.; Parker, T. M.; Gowda, D. C.; Urry, D. W. Biopolymers 1992, 32, 1251–1261.
41. Frank, H. S. J Chem Phys 1945, 13, 478–492.
42. Searle, M. S.; Williams, D. H. J Am Chem Soc 1992, 114, 10690–10697.
43. Searle, M. S.; Williams, D. H.; Gerhard, U. J Am Chem Soc 1992, 114, 10697–10704.
44. Tanford, C. The Hydrophobic Effect: Formation of Micelles and Biological Membranes; Wiley: New York, 1973.
45. Chang, D. K.; Venkatachalam, C. M.; Prasad, K. U.; Urry, D. W. J Biomol Struct Dyn 1989, 6, 851–858.
46. Thomas, G. J., Jr.; Prescott, B.; Urry, D. W. Biopolymers 1987, 26, 921–934.
47. Gosline, J. M. Biopolymers 1978, 17, 697–707.
48. Gosline, J. M.; French, C. J. Biopolymers 1979, 18, 2091–2103.
49. Gosline, J. M.; Yew, F. F.; Weis-Fogh, T. Biopolymers 1975, 14, 1811–1826.
50. Hoeve, C. A. J.; Flory, P. J. Biopolymers 1974, 13, 677–686.
51. Bykov, S. B.; Lednev, I. K.; Ianoul, A.; Mikhonin, A. V.; Asher, S. A. Appl Spectrosc 2005, 59, 1541–1552.
52. Manning, M. C.; Woody, R. W. Biopolymers 1991, 31, 569–586.
53. Ahmed, Z.; Asher, S. A. Biochemistry 2006, 45, 9068–9073.
54. Biron, Z.; Khare, S.; Samson, A. O.; Hayek, Y.; Naider, F.; Anglister, J. Biochemistry 2002, 41, 12687–12696.
55. Foster, J. A.; Bruenger, E.; Rubin, L.; Imberman, M.; Kagan, H.; Mecham, R.; Franzblau, C. Biopolymers 1975, 15, 833–844.
56. Tamburro, A. M.; Guantieri, V.; Daga-Gordini, D.; Abatangelo, G. J Biol Chem 1978, 253, 2893–2894.
57. Dorman, D. E.; Torchia, D. A.; Bovey, F. A. Macromolecules 1973, 6, 80–82.
58. Garrett, R. H.; Grisham, C. M. Biochemistry; Saunders College Publishing: Philadelphia, PA, 1999.
59. Caswell, D. S.; Spiro, T. G. J Am Chem Soc 1987, 109, 2796–2800.
60. Ahmed, Z.; Myshakina, N. S.; Asher, S. A. manuscript in preparation.
61. Takeuchi, H.; Harada, I. J Raman Spectrosc 1990, 21, 509–515.
62. Jordan, T.; Mukerji, I.; Wang, Y.; Spiro, T. G. J Mol Struct 1996, 379, 51–64.
63. Chen, X. G.; Li, P.; Holtz, J. S. W.; Chi, Z.; Pajcini, V.; Asher, S. A.; Kelly, L. A. J Am Chem Soc 1996, 118, 9716–9726.
64. Pajcini, V.; Asher, S. A. J Am Chem Soc 1999, 121, 10942–10954.
65. Asher, S. A.; Ianoul, A.; Mix, G.; Boyden, M. N.; Karnoup, A.; Diem, M.; Schweitzer-Stenner, R. J Am Chem Soc 2001, 123, 11775–11781.
66. Lazarev, Y. A.; Grishkovsky, B. A.; Khromova, T. B. Biopolymers 1985, 24, 1449–1478.
67. Li, P.; Chen, X. G.; Shulin, E.; Asher, S. A. J Am Chem Soc 1997, 119, 1116–1120.
68. Chi, Z.; Chen, X. G.; Holtz, J. S. W.; Asher, S. A. Biochemistry 1998, 37, 2854–2864.
69. Mikhonin, A. V.; Ahmed, Z.; Ianoul, A.; Asher, S. A. J Phys Chem B 2004, 108, 19020–19028.
70. JiJi, R. D.; Balakrishnan, G.; Hu, Y.; Spiro, T. G. Biochemistry 2006, 45, 34–41.
71. Chourpa, I.; Ducel, V.; Richard, J.; Dubois, P.; Boury, F. Biomacromolecules 2006, 7, 2616–2623.
72. Cook, W. J.; Einspahr, H.; Trapane, T. L.; Urry, D. W.; Bugg, C. E. J Am Chem Soc 1980, 102, 5502–5505.
73. Avbelj, F.; Baldwin, R. L. Proc Natl Acad Sci USA 2003, 100, 5742–5747.
74. Wang, Y.; Purrello, R.; Jordan, T.; Spiro, T. G. J Am Chem Soc 1991, 113, 6359–6368.
75. Lee, S.-H.; Krimm, S. Biopolymers 1998, 46, 283–317.
76. Overman, S. A.; Thomas, G. J., Jr. Biochemistry 1995, 34, 5440–5451.
77. Overman, S. A.; Thomas, G. J., Jr. Biochemistry 1998, 37, 5654–5665.
78. Overman, S. A.; Thomas, G. J., Jr. J Raman Spectrosc 1998, 29, 23–29.
79. Mikhonin, A. V.; Bykov, S. V.; Myshakina, N. S.; Asher, S. A. J Phys Chem B 2006, 110, 5509–5518.
80. Mikhonin, A. V.; Asher, S. A. J Phys Chem B 2005, 109, 3047–3052.
81. Ahmed, Z.; Illir, A. B.; Mikhonin, A. V.; Asher, S. A. J Am Chem Soc 2005, 127, 10943–10950.
82. Lednev, I. K.; Karnoup, A. S.; Sparrow, M. C.; Asher, S. A. J Am Chem Soc 1999, 121, 8074–8086.
83. Perry, A.; Stypa, M. P.; Foster, J. A.; Kumashiro, K. K. J Am Chem Soc 2002, 124, 6832–6833.
84. Ohgo, K.; Ashida, J.; Kumashiro, K. K.; Asakura, T. Macromolecules 2005, 38, 6038–6047.
85. Shi, Z.; Olson, C. A.; Rose, G. D.; Baldwin, R. L.; Kallenbach, N. R. Proc Natl Acad Sci USA 2002, 99, 9190–9195.
86. Schweitzer-Stenner, R.; Eker, F.; Griebenow, K.; Cao, X.; Nafie, L. A. J Am Chem Soc 2004, 126, 2768–2776.
87. Stapley, B. J.; Creamer, T. P. Protein Sci 1999, 8, 587–595.

Reviewing Editor: Laurence Nafie